

**FURTHER OBSERVATIONS ON V-4Cr-4Ti PRESSURIZED CREEP TUBES**—D. S. Gelles, R. J. Kurtz, M. B. Toloczko, and L. E. Thomas (Pacific Northwest National Laboratory)\*

## **OBJECTIVE**

The objective of this effort is to continue microstructural examinations of creep tubes to determine the deformation processes controlling thermal creep in vanadium alloys for comparison with creep response under irradiation.

## **SUMMARY**

Further observations are provided for pressurized thermal creep tubes of V-4Cr-4Ti examined following testing in the range 650 to 800°C for tests lasting up to  $\sim 10^4$  h. Precipitate particles have been analyzed by EELS to define interstitial contents, and are shown to be either C or O rich with only minor N contents. Grain shape aspect ratios as a function of strain have been measured and these data shows shape change as a result of effective mid-wall strains as high as 12.7%. Deformation mechanisms are considered to explain Newtonian viscous flow response at 800°C below effective midwall stresses of 70 MPa, and it is concluded that grain boundary sliding probably is the predominant mechanism based on the microstructural information presented here, but there is evidence that Harper-Dorn creep may also be a contributing creep mechanism under these conditions.

## **PROGRESS AND STATUS**

### **Introduction**

In our previous report on V-4Cr-4Ti pressurized creep tube examinations, [1] calculations suggested that nitrogen contamination may be responsible for increased precipitation of (Ti,V) oxy-carbo-nitride precipitates during testing. Increased precipitation near the outer surface extending inwards a distance of 30 and 70  $\mu\text{m}$ , respectively, was found at 650 and 700°C after  $\sim 10^4$  h and across the entire tube wall thickness at 800°C, and may have affected creep response. Also, the mechanism controlling creep behavior at higher stresses and lower temperatures was shown to most likely be viscous glide controlled creep arising from the presence of Ti and Cr solid solution hardening. The mechanism controlling behavior at lower stresses and higher temperatures could be grain boundary sliding or Coble creep, but given evidence for extensive dislocation production and rearrangement, an alternate explanation of Harper-Dorn creep was possible. The purpose of the present effort is to give further consideration to these issues. Electron energy loss spectroscopy (EELS) is applied to precipitates in specimen AR13 tested at 700°C and 119 MPa effective midwall stress for 9663 h and grain shape aspect ratios and precipitate particle distributions were examined to investigate applicability of Nabarro-Herring, Coble, Harper-Dorn creep or grain boundary sliding deformation mechanisms.

### **Experimental Procedure**

Specimens selected for further examination are listed in Table 1. Detailed information on specimen preparation and creep testing procedures were reported previously [2,3]. One of the tubes failed during testing, and therefore, the applied stress was removed while at temperature. The vacuum furnace was shut down immediately upon detecting a tube failure so the time at temperature in the unstressed condition was minimal. The other two tubes did not fail and were allowed to cool while still under pressure. A section of as-received tubing was heated treated at 1000°C for 1 h (designated AR) to provide comparison with deformed microstructures.

---

\*Pacific Northwest National Laboratory (PNNL) is operated for the U.S. Department of Energy by Battelle Memorial Institute under contract DE-AC06-76RLO-1830.

Table 1. Test conditions for specimens examined in this report

Specimen ID	Test Temperature (°C)	Midwall Effective Stress (MPa)	Time to failure (h)	Effective mid-wall strain (%)	Comments on failure
AR	Not tested				
AR02	650	200	10601	8.9	Burst
AR13	700	119	9663*	2.3	Did not fail
AR20	800	48	6052*	12.7	Did not fail

\*Specimen did not fail. The time listed is the total time at temperature.

Optical metallography was repeated using a hydrofluoric-nitric acid etch (15 ml lactic acid, 15 ml HNO<sub>3</sub>, and ~ 1 ml HF for ~ 1.5 min.) in order to better define grain boundary structure and (25 ml H<sub>2</sub>O, 12.5 ml HNO<sub>3</sub>, 12.5 ml HF for ~ 1 min [4]) to show precipitate stringers.

Specimen preparation for EELS analysis used a cross-section procedure, requiring dimple grinding and ion milling on a Gatan precision ion polishing system operating with 5 KeV argon ions. EELS was performed on a JEOL 2010F transmission electron microscope (TEM) operating at 200 KeV and equipped with a Gatan parallel EEL spectrometer.

## Results

### Metallography

In an effort to differentiate between different creep mechanisms, grain aspect ratio change was investigated. Figure 1 provides examples of the grain shapes in specimens AR, AR02, AR13, and AR20. All of the grain structures in these specimens appear equiaxed, with only a few examples of acicular grains elongated in the radial direction. It can be noted from Table 1, that effective midwall strains were 8.9, 2.3, and 12.7% respectively; however corresponding differences in grain elongation in the tube tangential direction are not apparent from these images.

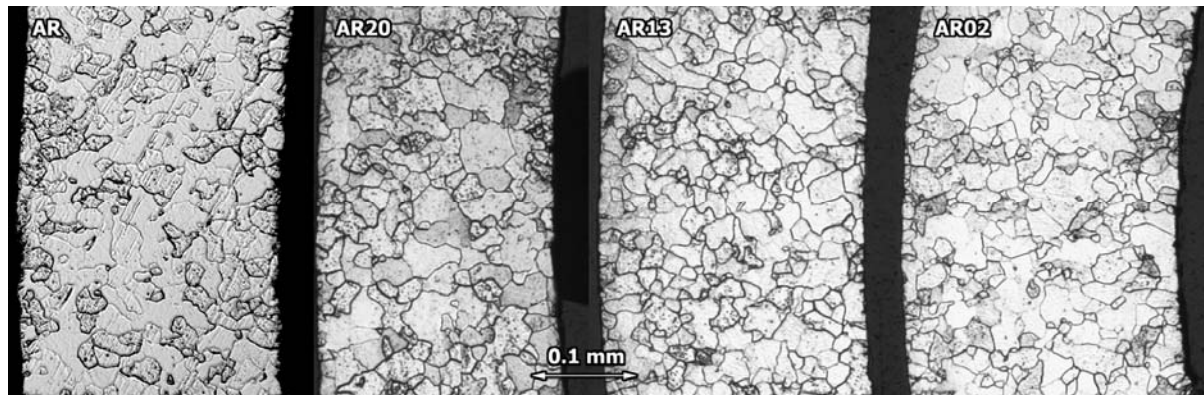


Fig. 1. Grain structure in V-4Cr-4Ti pressurized creep tubes.

A longitudinal section of specimen AR20 was examined following etching both to show grain structure and precipitate stringers [5] in order to determine if stringers could be used as markers to differentiate between operating creep mechanisms [6,7]. It should be noted that the longitudinal section is the only one that shows stringers but it is not ideal for differentiating between creep mechanisms because creep tubes show negligible change in length. Few well defined stringers were found and only one extended over several grains. It is shown in Fig. 2. The stringer does not appear to show any off-set due to grain boundary sliding or diffusional creep processes, suggesting that Harper-Dorn creep is more likely [7].

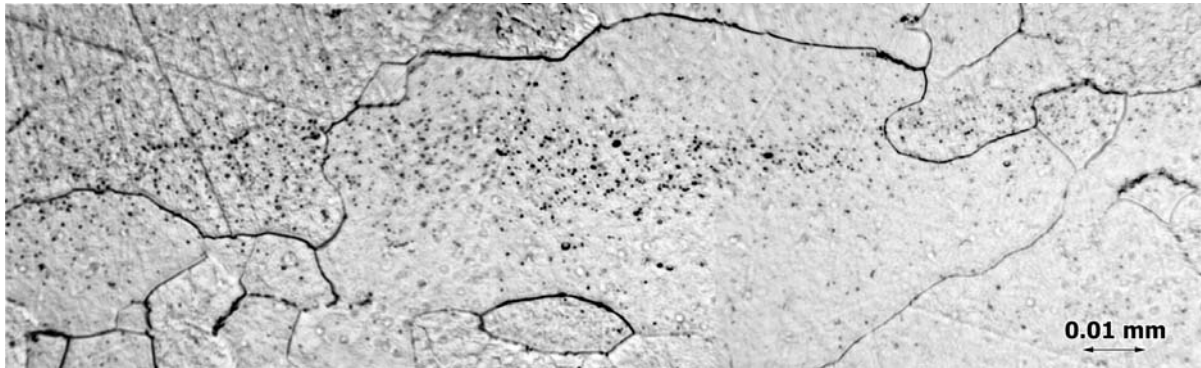


Fig. 2. Longitudinal stringer in specimen AR20.

It the course of examining for stringers in the longitudinal section of specimen AR20, several examples were found where precipitate particles appeared to collect on grain boundaries oriented in the longitudinal direction, whereas few boundaries oriented in the radial direction showed precipitate decoration. As hoop strain results in wall thinning, those boundaries oriented longitudinally would collect particles by diffusion processes involving grain boundaries. Four examples are provided in Fig. 3. Therefore, during creep at 800°C in specimen AR20, a diffusional process involving either bulk or grain boundary diffusion would need to operate for particles to collect as observed.

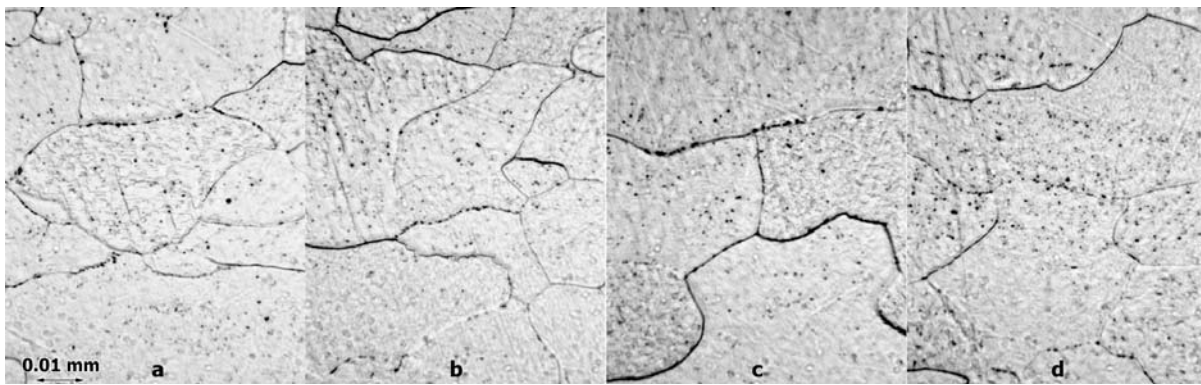


Fig. 3. Precipitation at grain boundaries in specimen AR20. The orientation is the same as in Fig. 2.

#### Analysis of grain aspect ratios

Grain aspect ratio measurements in tube radial and circumferential directions were made based on images similar to Fig. 1. Evidence for grain aspect ratio change was found as shown in Fig. 4. Note the bars bracketing the average values (open squares) for each specimen represent the range of measured aspect ratios and do not represent measurement error. It is noteworthy that the grain aspect ratio decreases approximately linearly with increasing midwall strain. In diffusion creep, the elongation of the grains will match the overall strain in the sample; whereas if deformation occurs predominantly by grain boundary sliding, there will be no significant grain elongation [7], so the grain aspect ratio will not change. The expected radial-to-circumferential aspect ratio can be estimated assuming none of the deformation is due to grain boundary sliding. As an example consider specimen AR20, which reached an effective mid-wall strain of 0.127. This is equivalent to a mid-wall hoop strain of 0.11. Since the longitudinal strain is zero for a pressurized creep tube and the radial strain is equal, but opposite in sign to the hoop strain the following equations give the predicted grain aspect ratio for AR20 after 12.7% deformation:

$$\begin{aligned}\varepsilon_c &= 0.11 = \ln\left(\frac{c}{c_o}\right) \\ \varepsilon_r &= -0.11 = \ln\left(\frac{r}{r_o}\right) \\ \frac{r}{c} &= \frac{r_o}{c_o} e^{-0.22} = 0.803 \frac{r_o}{c_o} = 0.803 * 1.10 = 0.88\end{aligned}\tag{1}$$

where  $r_o/c_o$  is the grain aspect ratio for the undeformed specimen. This calculation suggests that grain boundary sliding contributes significantly to the deformation of the specimen since the measured aspect ratio for AR20 is 1.02. As shown in Fig. 4, similar results were obtained for AR02 and AR13 suggesting grain boundary sliding may also contribute some fraction of the overall deformation for these specimens as well.

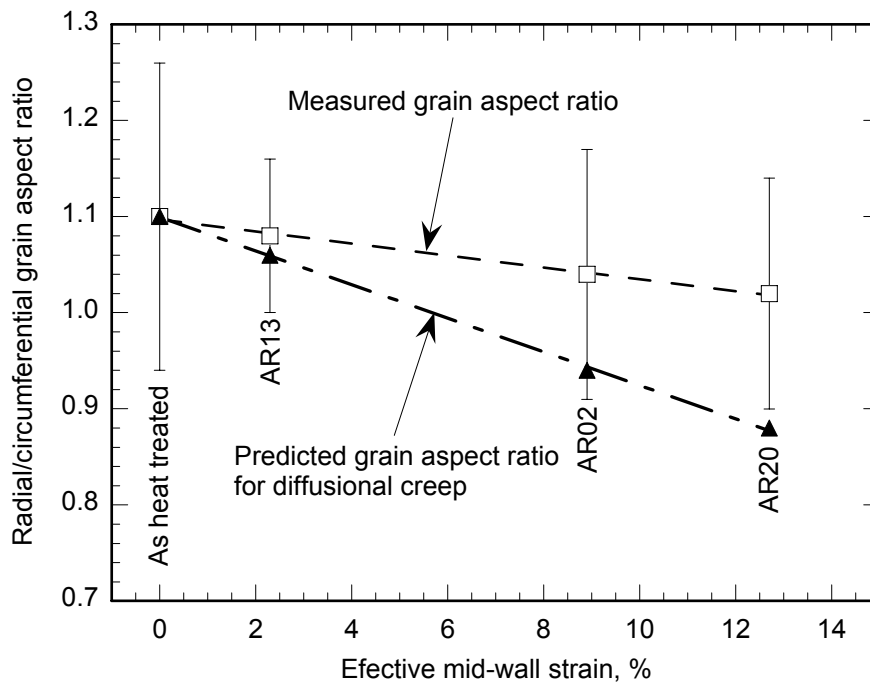


Fig. 4. Measured and predicted grain aspect ratio in pressurized creep tubes as a function of effective mid-wall strain.

#### Precipitate Interstitial contents from EELS

Precipitate particles in thinned regions of specimen AR13 near the outer diameter were analyzed using electron energy loss spectroscopy (EELS). Results for the first 15 particles analyzed are shown in Fig. 5. Typical energy loss spectra are only shown for the matrix, particle 2 and particle 3, and all spectra are provided using second difference analysis so that edges appear as ringing signals, with the relative size of the peak proportional to the height of the edge. The peak locations for V, Ti, C, N, and O are indicated.

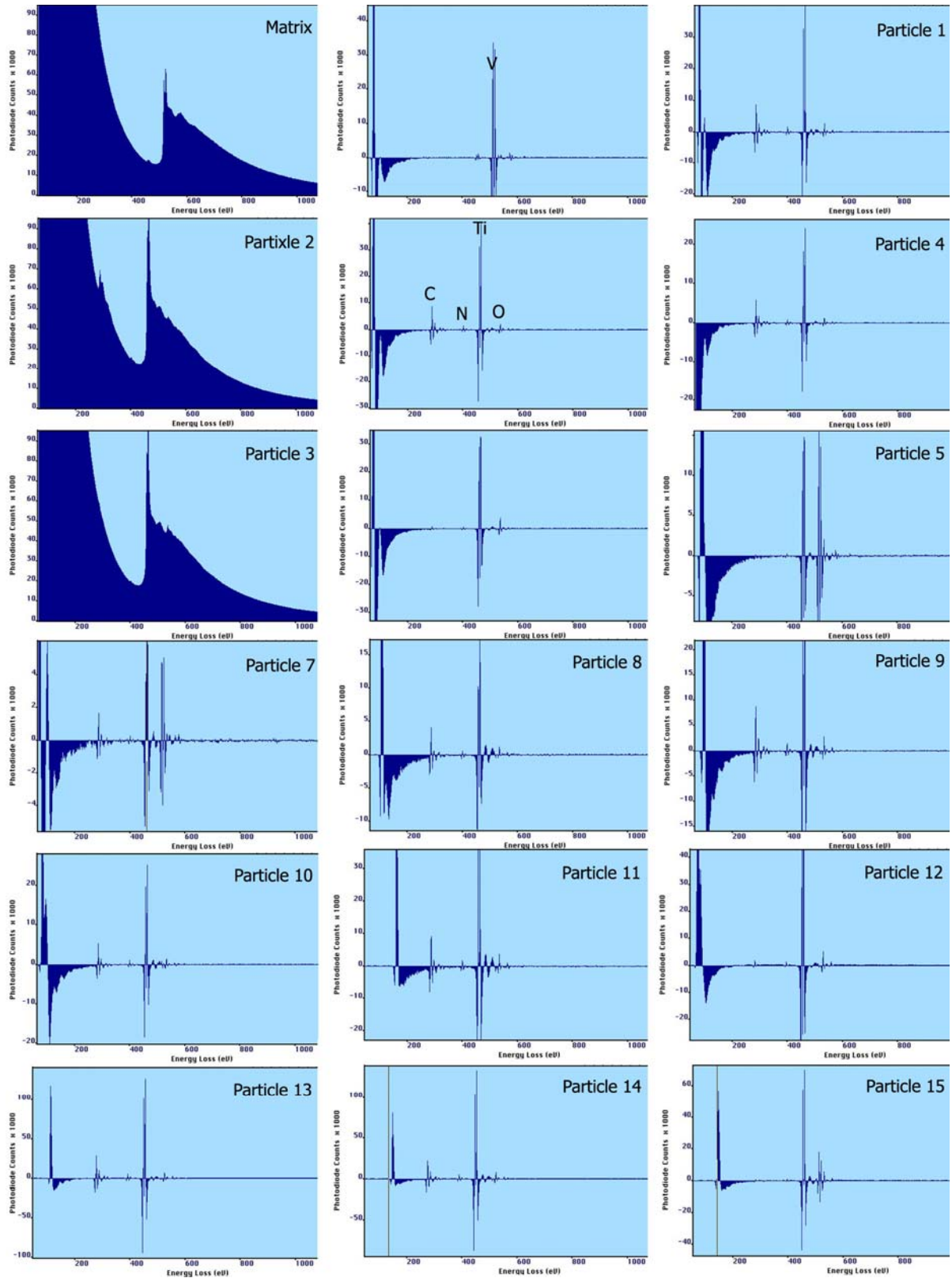


Fig. 5. EELS results for particles near the outer diameter of V-4Cr-4Ti creep tube AR13.

For the matrix spectrum, the large edge denotes V, and smaller edges correspond to Ti and Cr, showing up on either side of the V edge in the second difference analysis. In comparison, second difference spectra of particles 1, 2, and 4 shows that all particles are carbon rich, with less O and even less N. Particle 3 is different, rich in O and showing only slight traces of C and N. Particle 5 appears to be high in Ti and V, with moderate O showing. Spectra for the remaining particles show similar response and similar results were obtained for another 10 particles. Therefore, there was no evidence found for nitrogen rich particles near the outer surface of specimen AR13. All particles examined appeared to be similar to those expected in the as-heat treated alloy [5]. These results conflict with predictions that V-4Cr-4Ti thermal creep tests may have been affected by the environment [1].

## Discussion

Our previous work has shown that V-4Cr-4Ti pressurized tubes tested at 800°C and low stress can deform at creep rates with a stress exponent near 1 (0.84) or Newtonian creep, and that the corresponding microstructure showed subgrain dislocation evolution indicative of significant dislocation motion and rearrangement during creep [1]. It was therefore suggested that grain boundary sliding or Coble creep might not be the operating creep mechanism. Figure 6 is provided to show creep response as a function of stress in order to emphasize the dependence on stress, and it is apparent that for stress conditions below  $2 \times 10^{-3} \sigma/G$ , behavior can be interpreted as linear or Newtonian. It can be noted that such behavior had previously been assumed to be due to Coble creep [8] and more recently, it was concluded that this linear response does not exist [9]. It is considered to be important to resolve these differences, because if Newtonian creep is misinterpreted, creep predictions will contain large errors at low stresses.

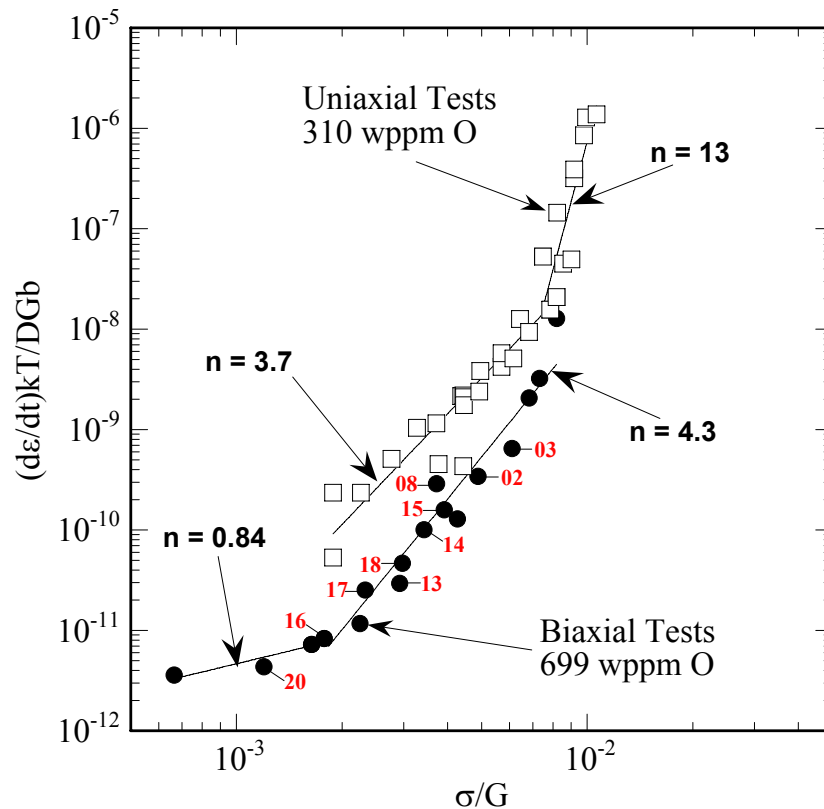


Fig. 6. Stress dependence of the normalized effective mid-wall creep strain for unirradiated vanadium alloys, with pressurized tube specimens chosen for microstructural examination identified by number.

All V-4Cr-4Ti pressurized tube specimen conditions examined by electron microscopy were found to show dislocation rearrangements due to applied stress. Table 2 summarizes the microstructural observations made on pressurized tubes and is organized with increasing test temperature and applied stress. It can be noted that higher stress conditions showed dislocation tangles and lower stress conditions developed examples of subgrain structure, understood to have developed by relaxation of deforming dislocations into lower energy configurations. From this information, it is apparent that specimen AR20 is behaving similarly to specimens tested at higher stress, and therefore it is reasonable to conclude that a dislocation mechanism such as Harper-Dorn creep is at least in part responsible for deformation during Newtonian response in this condition.

Table 2. Summary of microstructural observations on V-4Cr-4Ti pressurized tubes

ID	T <sub>test</sub> (°C)	( $\sigma/G$ ) x 10 <sup>-3</sup>	Strain (%)	Time (h)	Microstructural Features
AR02	650	4.876	9	1060	Complex dislocation tangles between fine precipitates.[1]
AR03	650	6.095	4.4	10,601	Complex dislocation tangles between fine precipitates.[1]
AR13	700	2.919	2.3	9963*	Moderate dislocation density with some subgrain structure.[1]
AR14	700	3.421	15	6667	Subgrain structure with low dislocation density in cells.[9]
AR15	700	3.912	13	2804	Complex dislocation tangles.[8]
AR08	725	3.714	> 5	1506	Moderate dislocation tangles with some fine precipitates.[1]
AR20	800	1.197	13	6052*	Subgrain structure with low dislocation density in cells.[1]
AR16	800	1.776	52	4029	Subgrain structure with low dislocation density in cells.[11]
AR17	800	2.329	14	864	Moderate dislocation tangles between fine precipitates.[10]
AR19	800	3.446	15	242	Moderate dislocation tangles between fine precipitates.[10]

\*Did not fail

The purpose of the grain aspect ratio and stringer study given in Figs. 1–4 was to differentiate between diffusion, grain boundary sliding and Harper-Dorn creep mechanisms as proposed by Langdon [6,7], but markers were not ideally oriented and were difficult to find. Based on stringer position across grain boundaries, Harper-Dorn Creep was indicated, but collection of particles on suitably oriented grain boundaries contradicted that conclusion and indicated either Nabarro-Herring or Coble creep was operating to some extent. Wang [12] has noted that Harper-Dorn creep should maintain a constant dislocation density irrespective of the operating stress, but the dislocation structures found in V-4Cr-4Ti pressurized tubes tested at 800°C and low stress developed a recovered dislocation structure containing subgrains. However, Cadek [13] has concluded that subgrain development should be possible only if the grain size exceeds the subgrain size applicable for the applied stress. In the case of the present experiments, the grain size (~ 20  $\mu\text{m}$ ) is larger than the predicted subgrain size,  $\lambda = 20b(G/\sigma) \approx 3 \mu\text{m}$ . It can be argued that grain boundary sliding must allow accommodation that may take the form of dislocation evolution, which may account for the subgrain structure observed. Alternately, it may be argued that subgrains can behave as internal grain boundaries producing Nabarro-Herring or Coble creep.

Consider instead prediction from theory. The normalized steady state creep rate can be written for Harper-Dorn, Nabarro-Herring, Coble creep and grain boundary sliding as follows:

$$\frac{\dot{\epsilon}kT}{DGb} = A \left( \frac{b}{d} \right)^p \left( \frac{\sigma}{G} \right)^n \quad (2)$$

where A is an appropriate dimensionless constant, D is the lattice diffusion coefficient, G is the shear modulus, b is the Burgers vector (0.262 nm for vanadium), k is Boltzmann's constant, d is the grain size (~ 20  $\mu\text{m}$ ), p is the appropriate grain size exponent, n is the stress exponent, and  $\sigma$  is the applied stress. The respective parameters are given in Table 3.

Table 3. Parameters for theoretical creep predictions

Parameter	Harper-Dorn	Nabarro-Herring	Coble	Grain Boundary Sliding
A	$1.4(\tau_p/G)^2$	27	54	106
p	0	2	3	2
n	1	1	1	1

Experimentally, the linear stress dependence is found to begin at a normalized stress level  $\sim 2 \times 10^{-3}$  for tests at 800°C, yielding a normalized strain of  $\sim 8 \times 10^{-12}$ . For Harper-Dorn the value of A depends upon the normalized Peierls stress,  $\tau_p/G$ , which can be estimated from the procedure given by Wang [12] as  $7.6 \times 10^{-5}$  at 800°C. Thus, the computed normalized creep strain at a stress of  $2 \times 10^{-3}$  for Harper-Dorn is  $1.6 \times 10^{-11}$ , for Nabarro-Herring it is  $9.3 \times 10^{-12}$ , for Coble creep it is  $2 \times 10^{-9}$ , and for grain boundary sliding creep it is  $3.6 \times 10^{-11}$ . The computed value for Nabarro-Herring creep is very close to the observed value in the biaxial creep tests, the computed creep rate for Coble creep is approximately 250 times larger than was observed, and the computed values for Harper-Dorn and grain boundary sliding creep are about 2–4 times higher than was observed. These calculations suggest that grain boundary sliding and Harper-Dorn creep mechanisms are more likely to describe pressurized tube creep behavior than Nabarro-Herring or Coble mechanisms since the Nabarro-Herring mechanism is considered to be operable only at very high homologous temperatures and the Coble model significantly over predicts the observed steady-state creep rate. On the other hand, the pressurized tube creep data may be significantly influenced by interstitial impurities remaining in solution such that comparisons with models that do not include such effects may be difficult to interpret.

In summary, evidence can be found for all three Newtonian creep mechanisms and grain boundary sliding contributing to creep in V-4Cr-4Ti at 800°C and low stress. Creep rate calculations predict Nabarro-Herring creep to be more favorable than Coble creep, but this seems unlikely at 800°C. Metallographic evidence shows precipitate pile-ups on favorably oriented grain boundaries in agreement with both diffusional creep mechanisms. Microstructural evidence indicates that grain boundary sliding and Harper-Dorn creep should operate, supported by the grain aspect ratio measurements and the observed dislocation production and rearrangement. Most likely, each of these mechanisms plays a role in the deformation process, as a function of distance from active grain boundaries.

## Conclusions

The mechanism controlling creep behavior at higher stresses/lower temperatures in V-4Cr-4Ti was shown to most likely be viscous glide controlled creep arising from the presence of Ti and Cr solid solution hardening. The predominant mechanism controlling creep behavior at lower stresses/higher temperatures should be grain boundary sliding or Coble creep, but given evidence for extensive dislocation production and rearrangement, Harper-Dorn creep may also contribute to the deformation process.

**References**

- [1] D. S. Gelles and R. J. Kurtz, DOE/ER-0313/36 (2004) 2.
- [2] R. J. Kurtz and M. L. Hamilton, DOE/ER-0313/25 (1999) 7.
- [3] R. J. Kurtz, A. M. Ermi, and H. Matsui in DOE/ER-0313/31 (2002) 7.
- [4] D. T. Hoelzer, ORNL, private communication.
- [5] D. T. Hoelzer and J. Bentley, 6<sup>th</sup> IEA and JUPITER Joint Workshop on Vanadium Alloys for Fusion Energy Applications, Tucson, Arizona, June 21–22, 2002.
- [6] T. G. Langdon, *Met. Trans.* 33A (2002) 249.
- [7] T. G. Langdon, *Mater. Sci. Eng. A283* (2000) 266.
- [8] M. Li and S. J. Zinkle, *J. ASTM Int.* 2(10) (2005), paper ID JA112462.
- [9] M. Li, T. Hagasaka, D. T. Hoelzer, M. L. Grossbeck, S. J. Zinkle, T. Muroga, K. Fukumoto, H. Matsui, and M. Narui, presented at the 12<sup>th</sup> International Conference on Fusion Reactor Materials.
- [10] D. S. Gelles, M. L. Hamilton, and R. J. Kurtz, DOE/ER-0313/26 (1999) 11.
- [11] D. S. Gelles, DOE/ER-0313/31 (2001) 17.
- [12] J. N. Wang, *Acta Mater.* 44 (1996) 855.
- [13] J. Cadek, *Creep in Metallic Materials*, *Mater. Sci. Monographs*, Elsevier (1988) 151.